Measurement 253 (2025) 117656

Contents lists available at ScienceDirect

Measurement

journal homepage: www.elsevier.com/locate/measurement

A review of laser-spectroscopy-based gas sensing techniques for trace formaldehyde detection

Xiu Yang [a,1], Baisong Chen [b,1], Yize Liang [b], Jiajia Hou [b], Dacheng Zhang [b], Biao Li [c], Angelo Sampaolo [d,e], Pietro Patimisco [d,e], Vincenzo Spagnolo [d,e,*], Xukun Yin [a,b,f,**]

[a] Hangzhou Institute of Technology, Xidian University, Hangzhou 311200, China
[b] School of Optoelectronic Engineering, Xidian University, Xi'an 710071, China
[c] Chongqing Key Laboratory of Optoelectronic Information Sensing and Transmission Technology, School of Optoelectronic Engineering, Chongqing University of Posts and Telecommunications, Chongqing 400065, China
[d] PolySense Lab—Dipartimento Interateneo di Fisica, University and Politecnico of Bari, Bari 70126, Italy
[e] PolySense Innovation srl, Via Amendola, 173, Bari 70126, Italy
[f] State Key Laboratory of Electrical Insulation and Power Equipment, Xi'an Jiaotong University, Xi'an 710071, China

ARTICLE INFO

Keywords:
Formaldehyde detection
Absorption spectroscopy
Trace gas sensors

ABSTRACT

Formaldehyde (H_2CO) is a colorless gas with a strong irritating odor, widely used in furniture manufacturing and house decoration. Already at concentration in the few ppm range, H_2CO represents great harm to human health, therefore, accurate measurement of formaldehyde concentration is of great significance for human safety. In this review, the laser-based spectroscopic techniques for formaldehyde gas detection were investigated, such as cavity ring-down spectroscopy (CRDS), cavity-enhanced absorption spectroscopy (CEAS), integrated cavity output spectroscopy (ICOS), tunable diode laser absorption spectroscopy (TDLAS), multi-pass cell absorption spectroscopy (MC), differential optical absorption spectroscopy (DOAS), non-dispersive absorption spectroscopy (NDAS), and photoacoustic spectroscopy (PAS). Among these techniques, the lowest detection limit achieved with an infrared laser source resulted in 28 ppt with a signal integration time of 40 s, and 210 ppt with an integration time of 30 s when using an ultraviolet light source.

1. Introduction

Formaldehyde (H_2CO) is a colorless gas with a strong pungent odor [1], mainly derived from the direct release and photochemical oxidation reaction of alkanes and nitrogen dioxide (NO_2), resulting as one of the most abundant aldehydes in the air [2]. It is easily soluble in water, alcohol and ether. Besides, it is an explosive, flammable, toxic and corrosive chemical gas [3]. H_2CO has been widely used in furniture manufacturing and house decoration, and a valid substitute for H_2CO has not yet been found [4]. Therefore, H_2CO is one of the most critical pollutants in new houses, and its accumulation in the indoor environment can exceed the limit imposed by the standard for human health [5]. H_2CO has been identified as a human carcinogen and teratogen by the World Health Organization (WHO), as well as one of the potentially strong mutagens [6]. The WHO requires that the concentration of H_2CO in residential areas must not exceed 80 part-per-billion (ppb) within 30 min [7]. According to American Conference of Governmental Industrial Hygienists (ACGIH) formaldehyde concentration should not exceed 300 ppb at any time. Therefore, the accurate measurement of the H_2CO concentration in the indoor environment is of great significance for human health. In addition, H_2CO has also been identified as a potential biomarker in human breath analysis. For example, in the breath exhaled by breast cancer patients, H_2CO concentration levels were observed to be approximately 1 part-per-million (ppm), whereas normal levels are typical at the level of several tens of ppb [8]. A sensitive and reliable human respiratory H_2CO analyzer can provide an effective method for non-invasive, real-time disease diagnosis and metabolic status monitoring.

At present, the main H_2CO detection methods include spectrophotometer [9,10], colorimetric [11], gas chromatography analysis [12],

* Corresponding author at: PolySense Lab—Dipartimento Interateneo di Fisica, University and Politecnico of Bari, Bari, 70126, Italy.
** Corresponding author at: School of Optoelectronic Engineering, Xidian University, Xi'an 710071, China
E-mail addresses: vincenzoluigi.spagnolo@poliba.it (V. Spagnolo), xkyin@xidian.edu.cn (X. Yin).
[1] These authors contributed equally to this work.

https://doi.org/10.1016/j.measurement.2025.117656
Received 23 December 2024; Received in revised form 3 April 2025; Accepted 20 April 2025
Available online 21 April 2025

electrochemical analysis [13], and so on. Among these sensing techniques, the spectrophotometer method needs to collect H_2CO and then treats it with iodine solution and sodium thiosulfate standard solution [14], which is not suitable for online, real-time measurement in industrial field. In 2022, C. Yuan et al. [15] achieved an ultimate H_2CO detection limit of 0.03 ppm by ultraviolet and visible (UV–vis) spectrophotometry in liquid media, but this method is limit to deal with H_2CO in liquid media, that is to say, H_2CO must undergo pre-treatment. The colorimetric method also needs to collect H_2CO and is not suitable for quantitative analysis. In 2024, F. Li et al. [16] realized a colorimetric sensor by using affordable and eco-friendly sodium alginate as a porous matrix, achieving a sensitivity of 0.02 ppb and a detection limit of 0.06 ppb, but the optimal detection time has reached 30 min. The gas chromatography analysis has high requirements for equipment, long processing time, cumbersome extraction and fussy operation steps and processes [17], thus not suitable for real-time detection. In 2019, H. Zhu et al. [18] achieved a H_2CO detection limit of 0.5 ppb with a signal-to-noise ratio of 6 based on heart-cutting 2-dimensional gas chromatography, but 11 min measurement duration makes it impossible to achieve real-time detection. The electrochemical analysis method cannot be applied to quantitative analysis, and suffers from interferences coming from other gas species. Besides, the poisoning phenomenon will occur with high H_2CO concentrations, leading to a failure of the monitoring. Moreover, electrochemical analysis requires large gas flow to be purged each time the device is turned on, in order to ensure the stability of the signal baseline [19]. In 2023, J. Chen et al. [20] developed a electrochemical sensor with a detection limit of 11 ppb (S/N = 3), but the calculated relative standard deviation has reached 3.6 % when testing 10 times in a 5 ppm H_2CO concentration. In conclusion, none of the above measurement methods can be efficiently use for on-site real-time detection of H_2CO.

With the rapid development of laser sources, several spectroscopic techniques based on the optical absorption started to growth, with the advantages of high sensitivity, good selectivity and fast response time [21–24], these optical techniques are currently used in several fields, such as atmospheric environment monitoring [25–27], industrial process control [28,29], non-invasive medical diagnosis [30–34], and life science. The most performant laser-based spectroscopic techniques [35–39] include cavity ring-down spectroscopy (CRDS) [40], cavity-enhanced absorption spectroscopy (CEAS) [41], integrated cavity output spectroscopy (ICOS) [42], tunable diode laser absorption spectroscopy (TDLAS) [43], multi-pass cell absorption spectroscopy (MC) [44], differential optical absorption spectroscopy (DOAS) [45], non-dispersive absorption spectroscopy (NDAS) [46] and photoacoustic spectroscopy (PAS) [47–49].

In this review, the most effect optical absorption techniques for H_2CO sensing will be classified and discussed in terms of the main figures of merit, namely the type of laser source, the ultimate detection limit and the signal integration time.

2. Formaldehyde absorption spectra

Laser-based absorption spectroscopic techniques are based on the Lambert-Beer law [50]:

$$I(\nu) = I_0(\nu) \cdot \exp(-\alpha(\nu) \cdot L), \quad (1)$$

where ν is the wavenumber of the incident wave, L is the optical path length of the gas cell, $I_0(\nu)$ is the incident laser light intensity, $I(\nu)$ is the light intensity transmitted by the absorption cell, $\alpha(\nu)$ is the absorption coefficient of the gas species, which can be expressed as:

$$\alpha(\nu) = N \cdot \sigma(\nu), \quad (2)$$

where N is the target gas molecule density, $\sigma(\nu)$ is the absorption cross-section of the gas species. The absorption cross-section represents the strength of the optical transition: thereby the choice of one of the strongest absorption features, possibly spectrally free from other interferents, determines the laser source to be used in the spectroscopic apparatus. The H_2CO molecule presents strong absorption lines from the ultraviolet to the infrared region. R. Meller et al. [51] measured the ultraviolet absorption cross sections of H_2CO in the wavelength range of 225–375 nm with a spectral resolution of 0.025 nm at a temperature of 298 K using a diode array detector. The spectral dependence of the H_2CO absorption cross section in the ultraviolet region is shown in Fig. 1, with a peak value of 7.23×10^{-20} $cm^2molecule^{-1}$ around 304 nm. Nevertheless, the NO_2 molecule is the main interference source in the ultraviolet spectral region (as also reported in Fig. 1), with broad spectral features in the range 320–360 nm [52].

The absorption coefficient of H_2CO in the infrared region are reported in the HITRAN database [53]. The strongest absorption features of H_2CO are in the wavelength range of 3200–4000 nm and 5250–6250 nm, as reported in Fig. 2. The specific absorption cross-sections of formaldehyde at 3.57 μm and 0.304 μm are 31.64×10^{-20} $cm^2molecule^{-1}$ and 7.23×10^{-20} $cm^2molecule^{-1}$, respectively.

The region centered at 3.55 μm apparently consists of different partially overlapping absorption features, giving rise to a broad, uneven band from 3.3 μm to 3.8 μm. Conversely, the spectral region at 5.7 μm shows the two well-defined P- and R-branch, separated by a somewhat intense central *Q*-branch with a peak value of 67.54×10^{-20} $cm^2molecule^{-1}$ around 5.73 μm, 2.1 and 9.3 times more intense of the peak value at 3.57 μm and 0.304 μm, respectively.

3. Laser-spectroscopy-based formaldehyde gas sensing techniques

A variety of laser-based absorption spectroscopic techniques for high-precision, real-time detection of H_2CO have been reported in literature, which are mainly divided into two categories, the direct absorption spectroscopy and the indirect absorption spectroscopy techniques [54]. Direct absorption spectroscopy obtains information, such as the gas species composing a mixture and its concentration, by comparing the spectral dependence of the light transmitted through the gas medium, $I(\nu)$, and the light incident on the gas cell, $I_0(\nu)$, according to the Lambert-Beer law (see Eq. (1). The most used spectroscopic techniques based on direct absorption are: CRDS, CEAS, ICOS, TDLAS, MC, DOAS and NDAS. Indirect absorption spectroscopy retrieves the same information on a gas sample by analyzing the energy released by

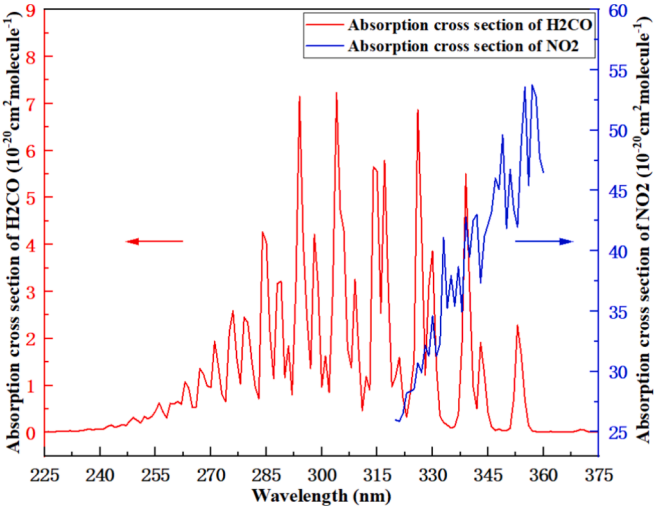

Fig. 1. The red line indicates the absorption cross section of H_2CO in the ultraviolet region of 225–375 nm. The blue line indicates the absorption cross section of NO_2 in the ultraviolet region of 320–360 nm. (For interpretation of the references to colour in this figure legend, the reader is referred to the web version of this article.)

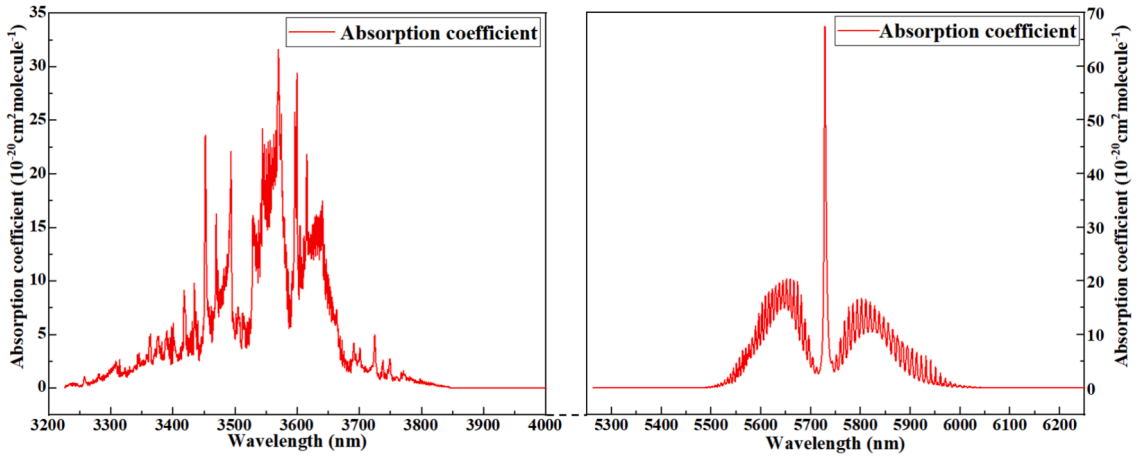

Fig. 2. Absorption coefficient of H_2CO in the infrared region of 3200–4000 nm and 5250–6250 nm.

gas molecules after the light absorption in the cell. The non-radiative relaxation of the excited molecules gives rise to the generation of both thermal waves, detected in photothermal spectroscopy, and acoustic waves, detected in conventional photoacoustic spectroscopy, and in its two variants, quartz-enhanced photoacoustic spectroscopy (QEPAS) and cantilever enhanced photoacoustic spectroscopy (CEPAS). As the discussion in the second section, formaldehyde has obvious absorption characteristics in both ultraviolet and infrared regions, and these absorption characteristics determine the choice of the light source band of laser-spectroscopy-based formaldehyde gas sensing techniques, which will be discussed below.

3.1. *Use of infrared light for formaldehyde gas sensing*

Fig. 2 shows the spectral dependence of the H_2CO absorption cross section in the infrared region, with a peak value of 67.54×10^{-20} cm^{2}molecule^{-1} around 5.73 μm, 2.1 and 9.3 times more intense of the peak value at 3.57 μm and 0.304 μm, respectively. Due to the obvious absorption characteristics in the infrared region, infrared light has been more widely used in the analysis of formaldehyde gas spectral characteristics than UV light. During our investigation, laser-spectroscopy-based formaldehyde gas sensing techniques using infrared light sources that have been reported are mainly divided into two categories, the indirect absorption spectroscopy and the direct absorption spectroscopy techniques, such as conventional PAS, QEPAS, CEPAS, CRDS, ICOS, DOAS, CEAS, TDLAS and MC.

3.1.1. *Indirect absorption spectroscopy*

Indirect absorption spectroscopy measures changes in a related property of the gas sample caused locally by the optical absorption, rather than directly measuring the absorption of light. The excited molecules relax the excess of energy in non-radiative pathways, generating a local thermal diffusion and a sound wave propagation. By correlating these changes with the concentration or characteristics of the analyte, indirect absorption spectroscopy can provide information about the sample composition, concentration, or other relevant properties [55].

Conventional PAS basically uses a resonant photoacoustic cell as gas cell, and a microphone placed at the antinode point of the sound wave pattern created within the cell at the resonant frequency. The laser beam passes though the PAS cell and the molecules of the analyte are excited and subsequently they relax. If the laser beam is intensity-modulated, the molecules will experience an alternation of excitation and no-radiative relaxation, generating a pressure wave propagating within the PAS cell. If the laser is intensity-modulated at the resonance frequency of the PAS cell, the sound wave will be amplified [56]. The amplified PAS signal amplitude is proportional to the Q-factor value of the photoacoustic cell. In addition, a PAS cell has the structure of a gas buffer, which can effectively reduce the influence of both the environment noise within the bandwidth of the PAS cell, and the optical noise caused by the window absorption [57]. In 2006, M. Angelmahr et al. [58] realized a PAS sensor for H_2CO detection by using a grazing-incidence optical parametric oscillator (GIOPO) pumped at a high repetition rate as the light source. The H_2CO absorption line of 2805.0 cm^{-1} was selected. A differential PAS cell was employed to effectively reduce electronic and acoustic noise, whose resonator tubes had an inside diameter of 5.5 mm and a length of 40 mm. The longitudinal acoustic resonance of the resonator tube was near 3.8 kHz. The final experimental results show that the detection limit of H_2CO is 3 ppb for a 3 s lock-in time constant at 3 min acquisition time.

QEPAS is a variant of PAS that uses a quartz tuning fork (QTF) to detect sound wave within the gas cell, instead of a microphone [59–62]. Therefore, the laser modulation frequency needs to be set to one of the resonant frequencies of the QTF or its sub-harmonics [63,64]. With the laser beam focused between the two prongs of the QTF, the generated acoustic wave causes the two QTF prongs to undergo natural oscillation motion, and a strain field is generated along the prongs, which in turn creates local changes in the quartz on the surface of the QTF [65–67]. These charges can be collected along the electrical contact deposited on the QTF prongs. As a result, the photoacoustic signal demodulated at the resonance frequency of the QTF, or one of its harmonics, will be proportional to the absorbing gas concentration. In 2004, M. Horstjann et al. [68] realized a QEPAS sensor with a continuous-wave mid-infrared DFB ICL as the light source for the detection and quantification of H_2CO. The QEPAS sensor is shown in Fig. 3. The detection module is composed by a standard 32.7 kHz-QTF with a *Q*-factor of 16725. The ultimate detection limit was 0.6 ppm with a 10 s signal integration time and a light power of 3.4 mW. The performance of a QEPAS sensor can be further improved by acoustically coupling the QTF with a pair of micro-resonator tubes and by lowering the QTF resonance frequency, keeping high its quality factor [69,70].

CEPAS is another variant of PAS that uses a cantilever as microphone [71]. The sound waves generated within the gas due to the photoacoustic effect will put the cantilever into vibration. The displacement field of the cantilever can be measured by a miniature Michelson interferometer, whose phase signal will be proportional to the concentration of the absorbing molecules. In 2013, C. B. Hirschmann et al. [72] introduced a sensitive H_2CO CEPAS sensor, as shown in Fig. 4. The CEPAS sensor uses a mid-infrared QCL as the light source tuned to H_2CO band at 1773.96 cm^{-1}. The PAS cell has a cylindrical shape with 4 mm diameter and 95 mm length. They reached an ultimate detection limit of 1.3 ppb with 1 s integration time.

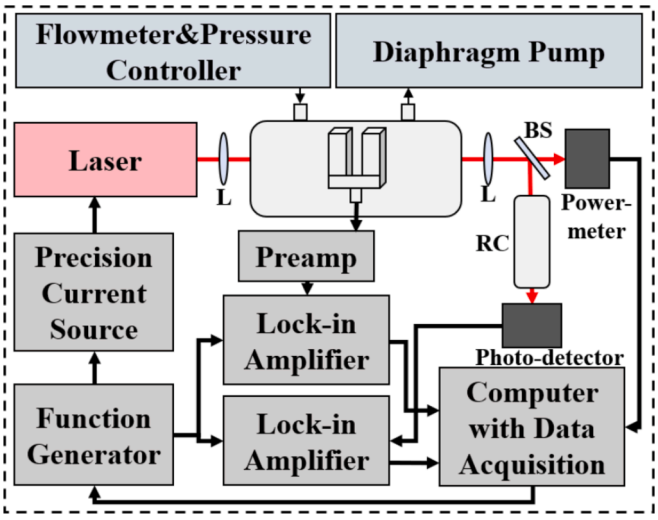

Fig. 3. The typical quartz-enhanced photoacoustic spectroscopy gas sensor system.

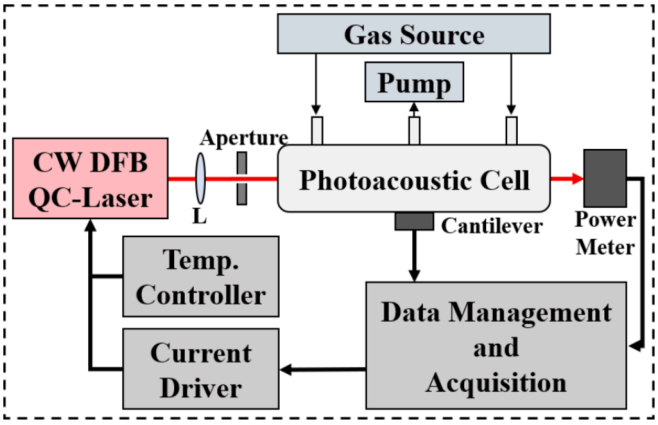

Fig. 4. The typical cantilever enhanced photoacoustic spectroscopy gas sensor system.

3.1.2. *Direct absorption spectroscopy*

As already discussed, in direct absorption spectroscopy, the attenuation of light is related to the properties of the gas species by means of the Beer-Lambert law (Eq. (1). For each spectral component of incident light, the intensity of the light passing through the gas absorption cell is measured. Then, the intensity of the light transmitted by the sample cell is also measured for the same spectral components. A direct comparison of both measurements allows the determination of the concentration of the absorbing gas species. Several direct absorption spectroscopy techniques that have been applied to H_2CO detection are described below.

CRDS is a highly sensitive gas sensing technique based on direct absorption first proposed in the late 1980 s [73]. The specific spectral component of the absorption coefficient of a gas species trapped in an optical cavity is calculated by measuring the ring-down rate (ring-down decay time) of the intensity of a light pulse which will decrease after every round trip in the cavity: the sum of the all contributions transmitted by the output mirror after each round trip gives rise to an exponential envelope of the light intensity that can be detected by a fast photodetector. The ring-down rate depends on the reflectivity of the ring-down cavity mirrors and the absorption coefficient of the gas medium in the cavity, but is independent to the incident light peak intensity. Therefore, the measurement result of the CRDS is not affected by fluctuations of the incident laser intensity, guaranteeing high sensitivity and low noise level [74]. In 2002, H. Dahnke et al. [75] used CRDS for H_2CO detection for the first time. The schematic diagram of the sensing system is depicted in Fig. 5. (a). This CRDS-based sensing system uses a tunable CO-overtone sideband laser at 3 μm as the light source. The reflectivity of both cavity mirrors is 99.954 % at 2850 cm^{-1}, which corresponds to the effective optical absorption intracavity path length of 1.2 km. A minimum detectable absorption coefficient of 7×10^{-9} cm^{-1} was estimated at an integration time of 1 s, which corresponds to a detection limit of 2 ppb in ambient air. In 2007, W. Zhou et al. [76] used an optical parametric oscillation (OPO) source for generating wide-tuned, narrow linewidth mid-infrared radiation from 2.2 to 4.0 μm in a CRDS setup for H_2CO detection near the absorption peak at 2914.46 cm^{-1}, schematically reported in Fig. 5. (b), resulting in a minimum detection limit of 72 ppb.

CEAS uses an optical cavity to increase the absorption path between the laser and the gas medium, thereby enhancing the interaction between them [77]. As in CRDS, the absorbing gas species is placed in a high-finesse optical cavity bounded, in the linear configuration, by two high reflective mirrors. Contrary to the CRDS method, here the absorption is calculated from the mirror-transmitted intensity. CEAS can achieve ultra-long optical paths allowing the boosting of the detection sensitivity [78]. One of the main drawbacks of CEAS is the locking of the laser mode to the optical cavity mode. In 2018, Q. He et al. [79] applied a Pound-Drever-Hall (PDH) locking technique in CEAS, which can lock the laser mode to optical cavity mode based on dual-feedback control. The PDH system structure is shown in Fig. 6. (a). The PDH mixes the signal of the function generator with the photodetector signal, and uses a low-pass filter to generate an error signal, which is further processed by the PID controller and fed back to the laser current driver for the frequency locking. On the other hand, the low-pass filter is also used to extract the amplitude of the error signal, to be sent to the PID controller, which drive the PZT controller for locking the cavity length to the laser mode. The optical cavity has an effective optical path length of 20 m with a cavity length of 2 cm, and a finesse of 1,572. By using the Allan-Werle variance analysis, a detection limit of 25 ppb with an averaging time of 1 s was obtained. It can be lowered down to 2.8 ppb when the averaging time increases to 200 s. In 2021, Q. He et al. [80] proposed a mid-infrared H_2CO detection system based on the coaxial mode-locked CEAS, sketched in Fig. 6. (b). The system uses a dynamic PDH locking system to periodically modulate the cavity length in a small range through low-frequency saw-tooth wave signal; as a result, the cavity resonant frequency changes slowly back and forth nearby the H_2CO absorption peak. A minimum detection limit of 52.8 ppb was achieved with an integration time of 1 s, reduced to 3.3 ppb with an integration time of 14 s.

ICOS involves trapping light within a high-finesse optical cavity, allowing for extended interaction between the light and the gas sample. As the gas absorbs specific wavelengths of light, the intensity of the transmitted light decreases, providing information about the gas concentration [81]. In 2006, J. H. Miller et al. [82] used the off-axis and integrated cavity output spectroscopy for H_2CO detection. The laser beam is directed into the cavity at a certain angle with respect to the cavity axis, which can increase the spectral density of cavity mode, thereby minimizing the noise in the absorption spectrum. As shown in Fig. 7. (a), the interband cascade laser (ICL) beam is directed into the ICOS gas cell and detected by a InSb detector. The ICL source provides a single mode, output power of 12 mW at 2832.8 cm^{-1}; the wavenumber can be tuned from 2831.8 to 2833.7 cm^{-1} by varying the ICL injection current at a fixed temperature. The H_2CO absorption line at 2832.483 cm^{-1} was targeted, achieving a minimum detection limit of 50 ppb at 3 s integration time. In 2022, G. Li et al. [83] firstly developed a highly sensitive real-time sensor to detect H_2CO in human exhaled breath based on wavelength modulation spectroscopy and off-axis integrated cavity output spectroscopy (WM-OA-ICOS). The system adopted a 5.85 μm quantum cascade laser (QCL) and an off-axis integrated cavity, as depicted in Fig. 7. (b), achieving a detection limit of 140 part-per-trillion (ppt) with an 88 s integration time. The experimental results of exhaled

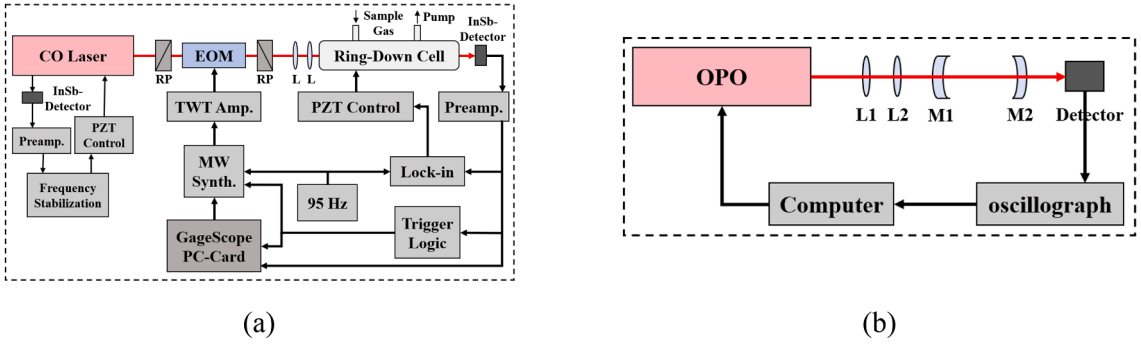

Fig. 5. The typical cavity ring-down spectroscopy gas sensor system.

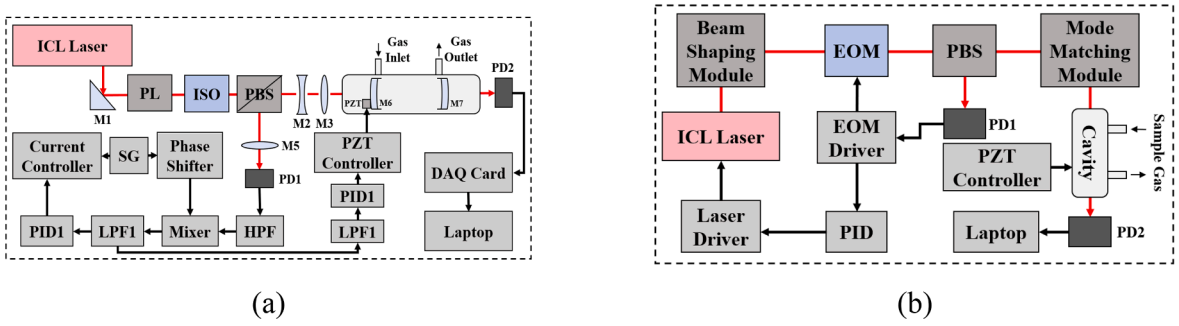

Fig. 6. The typical cavity-enhanced absorption spectroscopy gas sensor system.

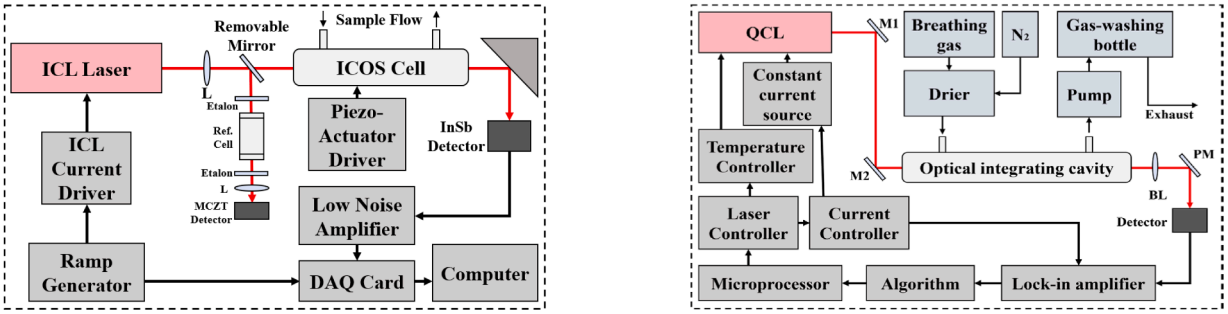

Fig. 7. The typical integrated cavity output spectroscopy gas sensor system.

gas showed relatively good differences, indicating the application prospect for early screening of lung cancer.

In DOAS, a light source with known spectral characteristics is directed through the gas sample. By comparing the spectrum of the incoming light with a reference spectrum measured when the optical pathlength is free of the gas of interest, DOAS can detect and quantify the concentration of trace gases based on the characteristic absorption features in the spectrum [84]. In 2007, C. Yang et al. [85] proposed a

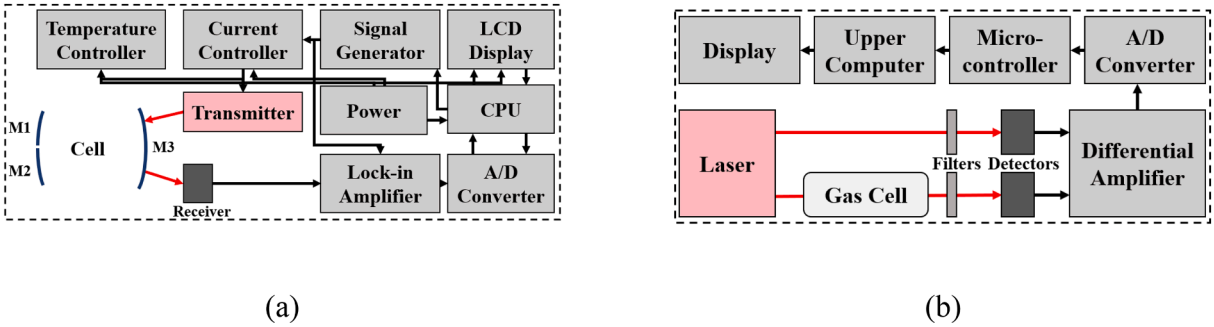

Fig. 8. The typical differential optical absorption spectroscopy gas sensor system.

DOAS sensor for indoor air quality detection, shown in Fig. 8. (a). They achieve highly sensitive monitoring of various indoor pollution gases such as H_2CO, NO_2, and SO_2. In 2017, M. Qin et al. [86] used a DOAS sensor, shown in Fig. 8. (b), for the real-time monitoring of indoor H_2CO concentration.

Our investigation shows that TDLAS is the most widely used among laser-spectroscopy-based formaldehyde gas sensing techniques, and almost all reported TDLAS technologies use infrared light sources. TDLAS operates by passing a laser beam through the sample gas, and the absorption of specific wavelengths of light by the gas molecules is measured. By tuning the laser's wavelength across absorption lines of the target gas, TDLAS can selectively detect and quantify the concentration of that gas in the sample. TDLAS technology can operate in amplitude modulation (AM), frequency modulation (FM) and wavelength modulation (WM) [87]. In AM spectroscopy, the intensity of the light source is modulated at a specific frequency, typically by means of an optical chopper. In WM and FM spectroscopy, the laser source is modulated in wavelength, typically by applying a sinusoidal modulation to the laser current. As the laser wavelength changes, it interacts with the sample gas, causing variations in the intensity of the transmitted light. The main difference between WM and FM is in the modulation frequency: WM uses modulation frequency in the kHz range, while FM in the MHz or even GHz range. In WM- or FM-TDLAS, the absorption cell containing the gas sample is usually a multipass cell (MC). A MC enhances the interaction between light and a sample by increasing the path length of the light through the sample. It typically consists of two mirrors arranged in a linear configuration. The laser beam passes through the gas sample multiple times, bouncing back and forth between the mirrors, effectively extending the path length, and enhancing the sensitivity of the TDLAS. The most used MC configurations are the White and the Herriott cell. Dense pattern multi-pass cells based on aberration theory [88] have been also recently proposed.

The White MC typically consists of a cylindrical chamber with multiple highly reflective mirrors arranged in a specific configuration. It employs spherical mirrors positioned at angles that allow light to be reflected multiple times within the chamber. This design minimizes optical aberrations and improves the uniformity of light distribution within the cell, enhancing the performance and accuracy of spectroscopic measurements. In 1989, G. W. Harris et al. [89] realized a TDLAS sensor for H_2CO detection with a White cell to improve the effective absorption optical path length up to 33.5 m optical path length. The scheme of the setup is reported in Fig. 9. (a). The experimental results showed a detection limit of 0.25 ppb with an integration time of 3 min. In 1999, P. Werle et al. [90] used the antimonide semiconductor laser with continuous-wave emission in the spectral range of 3–4 μm as the light source of the TDLAS system and a White cell to increase the absorption pathlength, as depicted in Fig. 9. (b). The Allan-Werle variance analysis reported a H_2CO detection limit of 120 ppt with 40 s integration time. In 1997, Y. Mine et al. [91] realized highly sensitive detection of H_2CO with a minimum detectable concentration of 30 ppb by using a multi-pass cell with an effective absorption path of 18.3 m and a mid-infrared light source with a central wavelength of 3.5 μm. The schematic diagram of the setup is shown in Fig. 9. (c). In 2016, K. Tanaka et al. [92] realized a compact multi-pass cell with a pair of cylindrical mirrors with an effective absorption path length of 9.8 m, used in a WM-TDLAS setup depicted in Fig. 9. (d) to targets the absorption line of H_2CO at 2979.663 cm^{-1}. They reached a detection limit of 73 ppb at 3 kPa. S. Li et al. [93] also designed a TDLAS sensing system using a White MC with an effective absorption path of 2.5 m in 2019. The system uses a tunable FP filter to simultaneously measure the absorption spectra of CH_4, H_2CO and CO_2 in the range of 3.1–4.4 μm. The experimental results showed a detection limit of 900 ppm for H_2CO concentration measurement.

The Herriott MC consists of two spherical mirrors positioned at each end of a cylindrical chamber. The mirrors are typically highly reflective, ensuring multiple reflections of the light within the chamber. The light enters the Herriott MC and undergoes multiple reflections between the two mirrors before exiting. The Herriott configuration effectively extends the path length of the light through the sample, enhancing the interaction between the light and the sample molecules. In 2000, D. G. Lancaster et al. [94] used a Herriott cell with an effective absorption optical path length of 100 m in a WM-TDLAS setup for H_2CO detection at

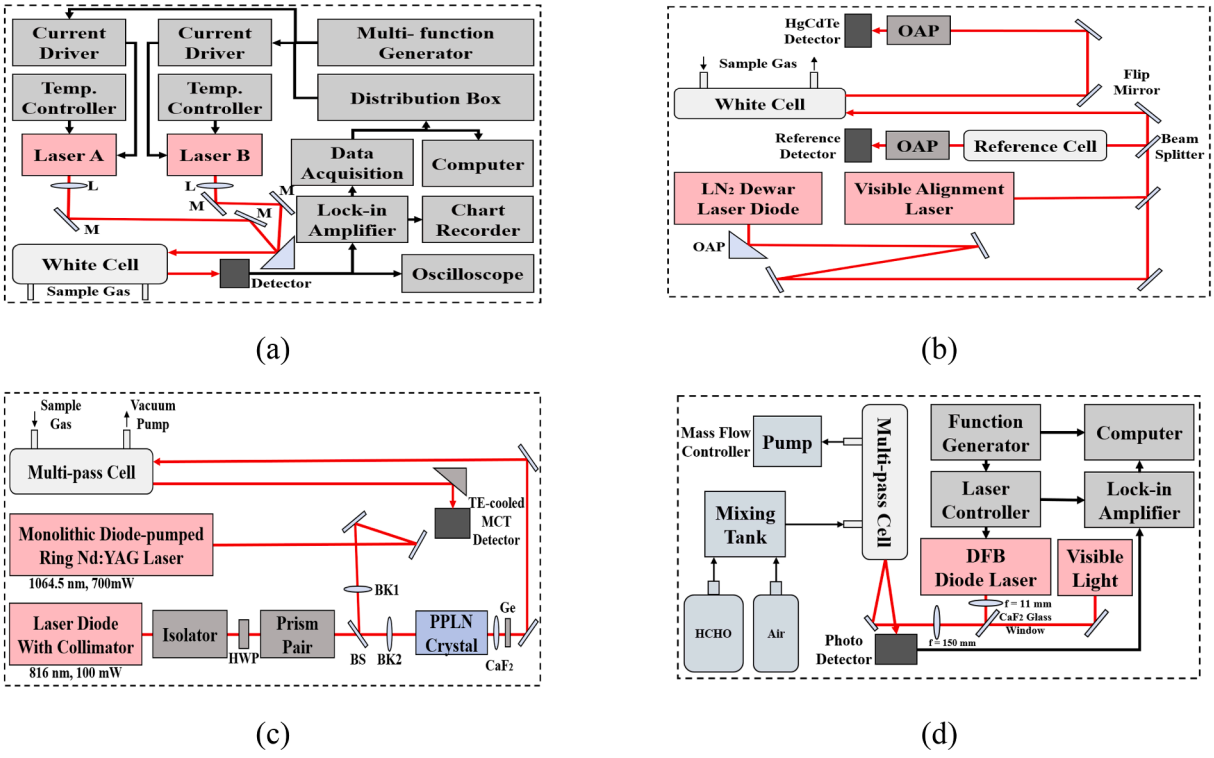

Fig. 9. The typical tunable diode laser absorption spectroscopy gas sensor system.

2831.64 cm^{-1}. The schematic diagram of the system is shown in Fig. 10. (a). The minimum detectable absorbance of H_2CO was in the 0.7–1.3 × 10^{-5} range at 40 Torr. In 2001, D. Rehle et al. [95] used an Herriott cell with an effective pathlength of 100 m to achieve a H_2CO detection limit of 0.32 ppb at an integration time of 20 s, with a setup sketched in Fig. 10. (b). In 2002, D. Richter et al. [96] also used a Herriott cell with an effective absorption optical path length of 100 m to detect H_2CO. The sensing system uses a mid-infrared laser source with a central wavelength of 3.5 μm as the excitation light source. A minimum detection limit of 74 ppt was achieved for a averaging time of 60 s. In 2014, J. Li et al. [97] realized a H_2CO sensor based on WM-TDALS by using a Herriott cell with effective absorption optical path length of 36 m. The system structure is shown in Fig. 10. (c). They reached a detection limit of 2.5 ppb detection in less than a 1 s integration time. In 2020, M. Winkowski et al. [98] described a H_2CO WM-TDLAS based sensor specially designed to detect cancer biomarkers in the air exhaled from human lungs. The schematic diagram of the system is shown in Fig. 10. (d). The system uses a Herriott cell with an effective absorption optical path length of 17.5 m to measure the H_2CO in the spectral range of 3595.77–3596.20 nm, with a minimum detection limit of 6.6 ppb.

A dense pattern MC employs an arrangement of mirrors to achieve a dense spot patterns and create a highly folded optical path within a relatively compact volume. As a result, a dense pattern MC allows to increase the mirror utilization rate and reduce the overall size of the multi-pass cell. In 2015, W. Ren et al. [99] designed a H_2CO WM-TDLAS based sensor using a dense pattern multi-pass cell with an effective absorption path length of 3.75 m, shown in Fig. 11. (a). By targeting the H_2CO absorption line at 2778.5 cm^{-1}, a minimum detection limit of the system of 6 ppb was obtained with a 1 s acquisition time, that can be lowered to 1.5 ppb by increasing the integration time up to 140 s. In the same year, L. Dong et al. [100] used a dense pattern multi-pass cell with an effective absorption path length of 54.6 m to detect H_2CO with WM-TDLAS approach. The schematic diagram of the system device is shown in Fig. 11. (b). The H_2CO detection limit was 2.5 ppb with the integration time of 1.5 s. In 2023, K. Duan et al. [101] proposed a battery-driven, portable optical gas sensor for ppb-level H_2CO diagnostics. The schematic diagram of the sensor system is shown in Fig. 11. (c). The system uses a mid-infrared ICL with a central wavelength of 3.6 μm as the light source, and a dense pattern multi-pass cell with the effective absorption path length of 26.4 m. The minimum detection limit of the system for H_2CO detection was 1.42 ppb with an integration time of 0.2 s. T. Wu et al. [102] also reported a trace H_2CO detection system using a dense pattern multi-pass cell as shown in Fig. 11. (d). The system used a quantum cascade laser (QCL) with a central excitation wavelength of 5.68 μm, targeting the absorption line of H_2CO at 1759.73 cm^{-1}. With an effective absorption optical path length of 67 m, a minimum detection limit of 28 ppt was reached with a 40 s integration time. The sensitivity can meet the requirements of the trace H_2CO detection in the atmospheric environment. In the same year, B. Fang et al. [103] achieved a detection limit of 650 ppt using a compact improved spherical mirror multi-pass cell with an optical absorption path length of 50.6 m. Notably, the optical case dimension of this sensor is just 46 × 28 × 16 cm^3, making it highly conducive to portable use and expanding its potential applications across diverse scenarios.

3.2. Use of UV light for formaldehyde gas sensing

Fig. 1 shows the spectral dependence of the H_2CO absorption cross section in the ultraviolet region, with a peak value of 7.23 × 10^{-20} $cm^2molecule^{-1}$ around 304 nm. In our investigation, laser-spectroscopy-based formaldehyde gas sensing techniques using UV light sources that have been reported are: conventional PAS, NDAS, CRDS, DOAS and CEAS. In 1988, M. Boutonnat et al. [104] first applied UV light to formaldehyde gas detection, who reported on an experimental scheme for quantitative measurement of H_2CO gas in a mixture of NO_2, CH_3CHO and N_2. The experimental setup is shown in Fig. 12. The system uses a tunable pulsed laser in the range of 300–310 nm as the light source, and the laser beam passes through the photoacoustic cell twice to increase the effective absorption optical pathlength. The photoacoustic signal is detected by a condenser microphone positioned radially. The experiment demonstrates a detection limit of 20 ppb for H_2CO at 303.59 nm.

J. J. Davenport et al. [105] also used UV light to detect H_2CO based

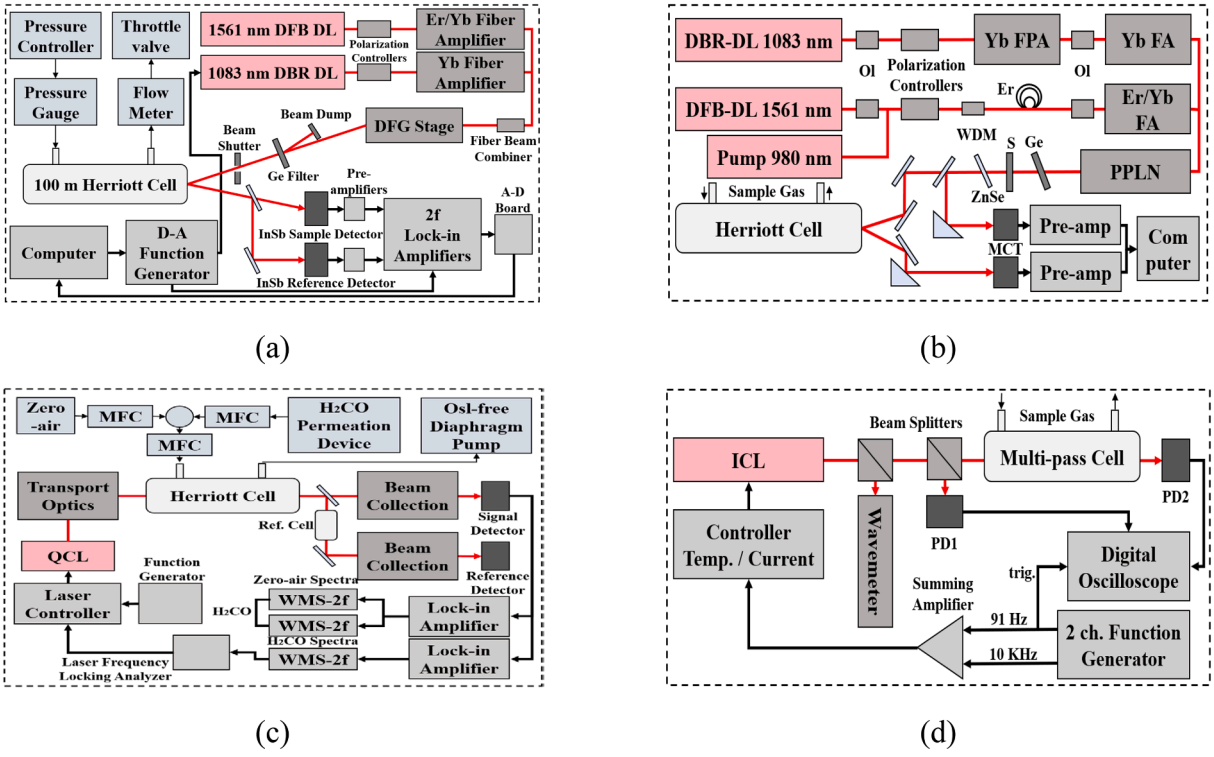

Fig. 10. The typical multi-pass cell absorption spectroscopy gas sensor system based on a Herriott cell.

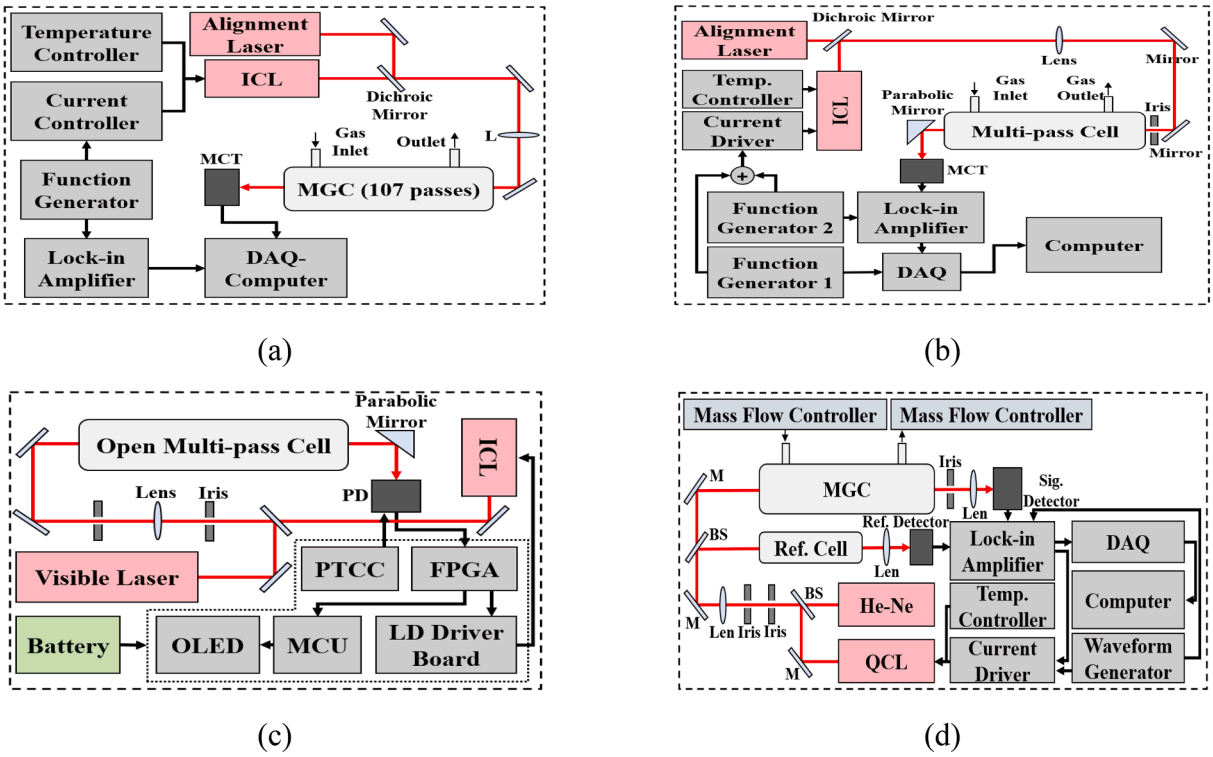

Fig. 11. The typical multi-pass cell absorption spectroscopy gas sensor system based on a dense pattern multi-pass cell.

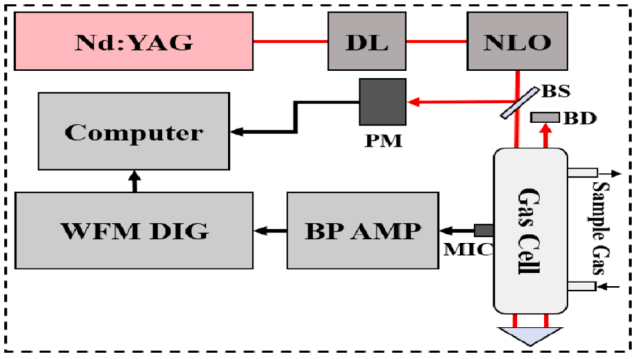

Fig. 12. The typical conventional resonant photoacoustic spectroscopy gas sensor system.

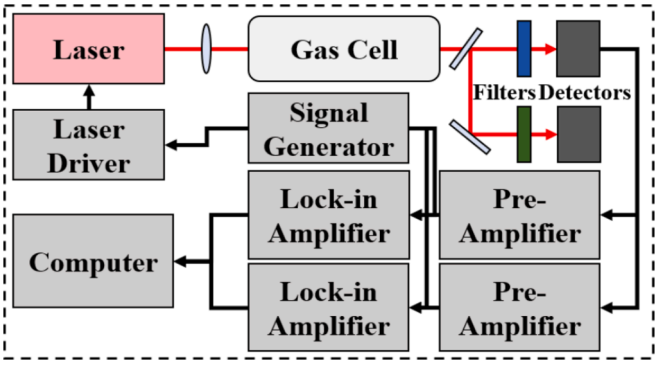

Fig. 13. The typical non-dispersive absorption spectroscopy gas sensor system.

on non-dispersive UV absorption spectroscopy (NDAS) in 2014. NDAS is a technique used to measure the concentration of gases in a sample based on their absorption of specific wavelengths of light. Unlike dispersive spectroscopy methods, which use prisms or diffraction gratings to separate light into different wavelengths, NDAS does not involve wavelength dispersion [106]. Transmission spectra of the absorbing gas species are obtained by optical filtering, i.e., by using an interference filter matched with the spectral region of the gas absorption feature. A reference channel is used to compensate for the influence of the intensity change of the light source, whose signal is obtained by using the interference filter matched with the spectral region with negligible optical absorption. The schematic of the setup designed by J. J. Davenport et al. [105] is shown in Fig. 13.

The system uses the H_2CO strong absorption peak at 339 nm as the effective signal and the negligible absorption region at 336 nm as the reference signal. The light source is a modulated UV LED: the desired spectral band is selected by means of a narrowband filter. A minimum detection limit of 6.6 ppm was reached with an integration time of 20 s. In the same year, P. Nau et al. [107] combined UV absorption spectroscopy with CRDS to achieve highly sensitive detection of H_2CO at 370 nm, reaching a minimum detectable mole fraction of 2×10^{-4}, at 1000 K and 33.3 mbar. In 2016, S. Shen et al. [108] used a DOAS sensor, reported in Fig. 14. (a), operating in the spectral range 313–341 nm to analyze H_2CO in an urban area of Shanghai in October 2013. In 2019, R. Sheng et al. [109] proposed an UV analyzer for H_2CO concentration detection based on DOAS technology too, shown in Fig. 14. (b). The gas cell used in the system can achieve an effective optical path length of 2 m, and data processing is combined with the least square method, which effectively improves the system performance in terms of signal-to-noise ratio analysis. The experimental results reported a detection limit for H_2CO detection as low as 0.09 ppm.

For further improvement of system's performance, R. A. Washenfelder et al. [110] and J. Liu et al. [111] both proposed a method based on broadband cavity-enhanced absorption spectroscopy (BBCEAS) in the UV spectral region. In 2016, R. A. Washenfelder et al. [110] proposed a detection scheme for simultaneous measurement of H_2CO and NO_2 based on broadband cavity-enhanced absorption spectroscopy (BBCEAS) in the UV spectral region. A sketch of the setup is

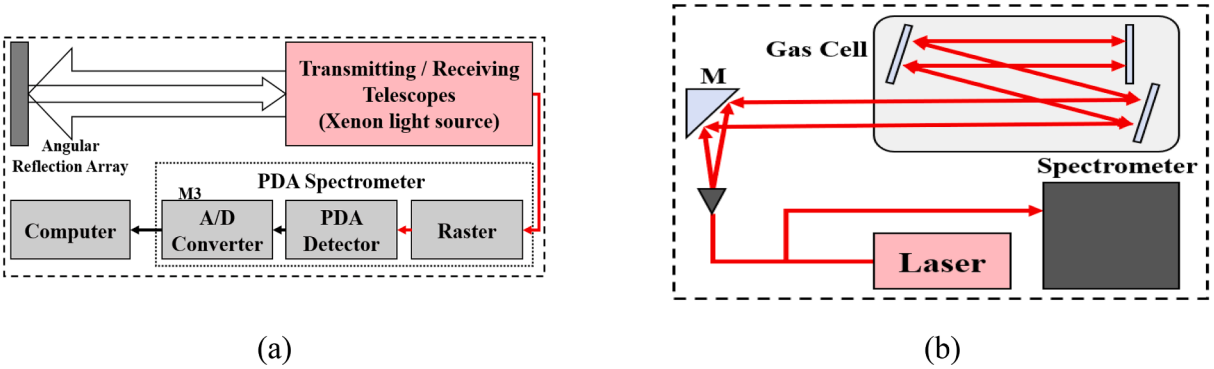

Fig. 14. The typical differential optical absorption spectroscopy gas sensor system.

shown in Fig. 15. (a). The output spectral range of the broadband light source was 170–2100 nm, and the optical cavity used reached an effective path length of 1.43 km. A grating monochromator and charge-coupled device array detector was used to measure the output signal of the cavity in the 315–350 nm spectral region. The experimental results demonstrated a linear response of the cavity output signal as a function of the analyte concentration, with detection limit for NO_2 and H_2CO of 140 and 210 ppt at 30 sec integration time, respectively. The use of a broadband light source opens up the possibility to detect a large variety of gas species exploiting also the build-up optical power of the cavity. On the same track, in 2020 J. Liu et al. [111] introduced the incoherent broadband cavity-enhanced absorption spectroscopy (IBBCEAS) technique based on UV light-emitting diode (LED) to measure H_2CO in ambient air. The layout of the optical cavity module is shown in Fig. 15. (b). The optical source consisted of two LEDs (325 and 340 nm) and a Y-type fiber bundle coupling output. The optical cavity had a length is 0.84 m, with an effective path length of 2.15 km at 350 nm. They reached a minimum detection limit of 380 ppt at an integration time of 30 s. The sensor was tested on-site in the Szechwan Basin, and the measurement results were compared with those obtained simultaneously by using a Hantzsch instrument (Mode, AL4021, Aerolaser GmbH, Garmisch-Partenkirchen, Germany), resulting in a good correlation ($R^2 = 0.769$).

4. Discussion

Table 1 summarizes the performance achieved for formaldehyde detection, such as detection limit, time resolution and normalized noise equivalent absorption coefficient (NNEA), by each spectroscopic technique previously discussed, where NNEA is measured in $cm^{-1}W/Hz^{-1/2}$ by normalizing the noise equivalent absorption to a 1 Hz measurement bandwidth [112].

Apart from excellent results obtained with CEAS and WM TDLAS, results clearly show that the optical techniques can easily reach sub-ppm detection of formaldehyde with signal integration times of a few seconds. Moreover, the selection of the H_2CO absorption line plays a crucial for the H_2CO ultimate performance. The H_2CO absorption lines selected by all sensors described in previous sections are listed in Table 2 and grouped in two classes, UV and infrared region, which is more intuitive in Fig. 16.

Fig. 16. shows detection limit achieved by different laser-spectroscopy-based formaldehyde gas sensing techniques, where different colors represent different technologies, and on the right side of the figure we further plot technologies with detection limit lower than 3 ppb.

It can be found that most of the optical sensors for H_2CO sensing measurement used absorption lines in the mid-infrared band. The main reason is that the technological development of infrared light sources is relatively mature, and the tunable mid-infrared light sources have shown better performance in terms of output power, long-term stability, and wavelength tunability. However, the use of a mid-infrared light source significantly impacts on the cost of the overall sensing system. The use of low-cost ultraviolet light source to realize H_2CO sensing measurement is also a valid option. Currently, the best detection limit reached with a low-cost, UV source was 210 ppt, obtained by R. A. Washenfelder et al. [110] by using the BBCEAS with a broad UV source emitting in the range 315–350 nm. In this spectral region, NO_2 is the only main absorption interferent species. If the balance between system cost and system performance can be achieved, laser-based absorption spectroscopic techniques will be more advantageous among formaldehyde gas sensing techniques.

The development trend of H_2CO optical absorption techniques is not only related to its cost, but more importantly, depends on the needs of its application scenarios and portability. For residential indoor H_2CO measurement, users prioritize affordability and compactness due to limited budgets and minimal technical expertise. In contrast, professional testing laboratories and industrial applications emphasize sensor performance. If the sensors are also portable, this will significantly

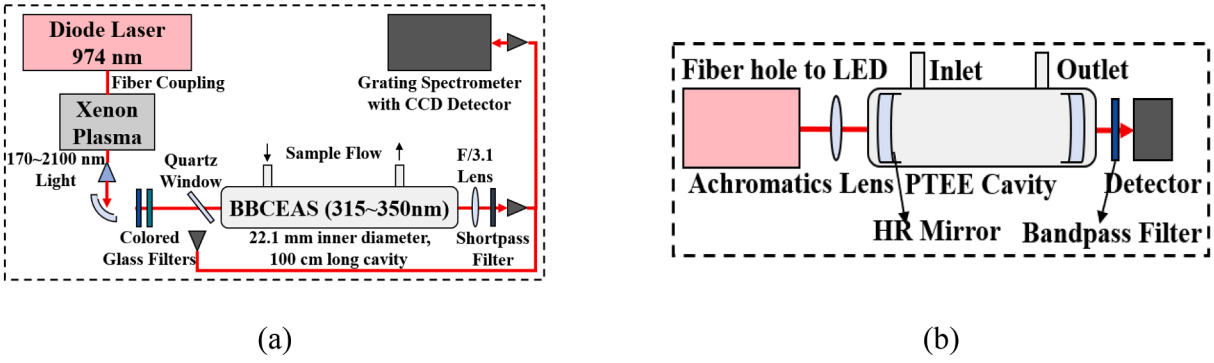

Fig. 15. The typical cavity-enhanced absorption spectroscopy gas sensor system.

Table 1
Comparison of performance achieved by different H_2CO measurement techniques.

Technique	Frequency cm^{-1}	Detection limit ppb	Time resolution s	NNEA $cm^{-1}W/Hz^{-1/2}$	Ref.
CRDS	2853.44	2	1	/	[75]
	2914.46	72	/	/	[76]
CEAS	28571.43–31746.03	0.21	30	/	[110]
	28011.2–30864.2	0.38	30	/	[111]
	2778.5	25	1	/	[79]
	2778.49	52.8	1	/	[80]
ICOS	2832.483	100	/	/	[82]
	1710.52	0.14	88	/	[83]
TDLAS/MC	1740	0.25	180	/	[89]
	2800.2	0.12	40	$1.57 \bullet 10^{-7}$	[90]
	2861.72	30	/	/	[91]
	2979.663	73	40	$2.32 \bullet 10^{-10}$	[92]
	2273–3226	900,000	40	/	[93]
	2831.64	0.2	1	/	[94]
	2832	0.32	20	/	[95]
	2857.14	0.074	60	/	[96]
	1759.73	2.5	1	/	[97]
	2780.71–2781.05	6.6	/	/	[98]
	2778.5	6	1	/	[99]
	2871	2.5	1.5	$3.29 \bullet 10^{-8}$	[100]
	2778.5	1.42	0.2	/	[101]
	1759.73	0.028	40	/	[102]
	2831.64	0.65	1	/	[103]
DOAS	20000–55555.56	90	120	/	[109]
NDAS	29498.53	6600	20	/	[105]
Conventional PAS	32939.16	20	/	/	[104]
	2805	3	3	$6.2 \bullet 10^{-9}$	[58]
QEPAS	2832.5	600	10	$2.2 \bullet 10^{-8}$	[68]
CEPAS	1773.959	1.3	1	$6.04 \bullet 10^{-10}$	[72]

Table 2
Classification of H_2CO absorption lines selected by different technologies.

Wavelength region	Technique	Selected absorption line
Infrared region	CRDS	3504.54 nm [75], 3431.17 nm [76]
	CEAS	3599.06 nm [79], 3599.08 nm [80]
	ICOS	3530.47 nm [82], 5846.17 nm [83]
	TDLAS/MC	5747.13 nm [89], 3571.17 nm [90], 3494.40 nm [91], 3356.08 nm [92], 3099.81–4399.47 nm [93], 3531.52 nm [94103], 3531.07 nm [95], 3500.00 nm [96], 5682.69 nm [97], 3595.77–3596.20 nm [98], 3599.06 nm [99101], 3483.11 nm [100], 5682.69 nm [102]
	DOAS	3607.00 nm [86]
	Conventional PAS	3565.06 nm [58]
	QEPAS	3530.45 nm [68]
	CEPAS	5637.11 nm [72]
Ultraviolet region	CRDS	370 nm [107]
	CEAS	315–350 nm [110], 324–357 nm [111]
	DOAS	313–341 nm [108], 180–500 nm [109]
	NDAS	339 nm [105]
	conventional PAS	303.59 nm [104]

enhance their operational efficiency. In 2023, B. Fang et al. [103] developed a H_2CO sensor with a dimension of only 46 × 28 × 16 cm^3 base on multi-pass cell absorption spectroscopy, achieving a remarkable detection limit of 650 ppt. Such a portable and high-performance H_2CO sensor is not only suitable for indoor and outdoor scenarios, but also can play a good role in the fields of professional testing laboratories and industrial applications. Regarding sensor portability, PAS offers distinct advantages. QEPAS, for instance, employs a quartz tuning fork as its sensing core, having a commercial standard dimension of just 6 mm × 1.4 mm × 0.2 mm with a resonance frequency of $f = 32760$ Hz and a Q-factor of 16725. This component enables compact sensor designs while maintaining high performance, a critical balance for portable instrumentation. Beyond these aforementioned applications, H_2CO sensor hold significant potential in the medical field, where exhaled formaldehyde levels serve as a biomarker for lung health. In 2022, G. Li et al. [83] developed an ICOS-based sensor capable of effectively detecting H_2CO in exhaled breath, demonstrating promising prospects for early screening of lung cancer. For medical applications, sensor performance and portability are pivotal benchmarks. By integrating high-sensitivity detection with compact design, laser-based H_2CO absorption spectroscopic techniques will demonstrate significant competitive advantages.

5. Conclusions

This work presents a critical review on the optical sensing techniques applied to H_2CO detection, including cavity ring-down spectroscopy (CRDS), cavity-enhanced absorption spectroscopy (CEAS), integrated cavity output spectroscopy (ICOS), tunable diode laser absorption spectroscopy (TDLAS), multi-pass cell absorption spectroscopy (MC), differential optical absorption spectroscopy (DOAS), non-dispersive absorption spectroscopy (NDAS), conventional resonant photoacoustic spectroscopy, quartz-enhanced photoacoustic spectroscopy (QEPAS) and cantilever enhanced photoacoustic spectroscopy (CEPAS). Among them, the best ultimate detection limits were achieved by using an infrared excitation light source, resulting in 28 ppt with a signal integration time of 40 s. Although the use of UV sources does not guarantee

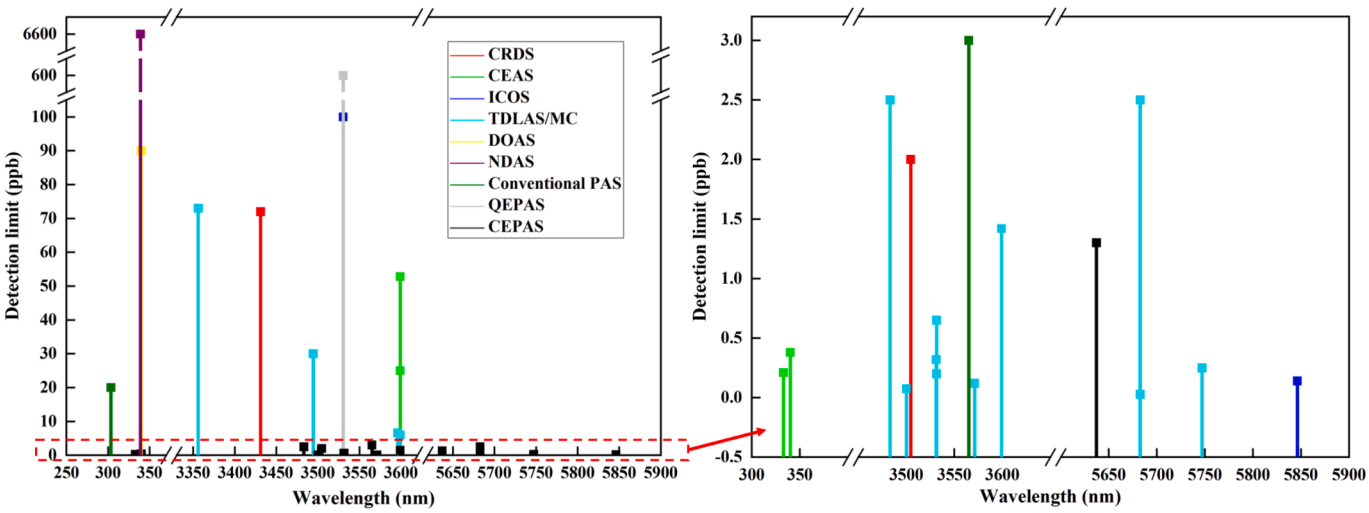

Fig. 16. Detection limit achieved by different laser-spectroscopy-based formaldehyde gas sensing techniques.

comparable performance with those obtained with infrared sources, H_2CO sensors based on UV source can still meet the requirement of sensitive measurement in the atmosphere. The main advantage of UV light sources is in the reduction both of the overall cost of the sensing system costs and of the system complexity, compared to the use of infrared light sources. Taking into account the performance, cost, and portability of the sensor comprehensively, laser-based absorption spectroscopic techniques will be suitable for use in various scenarios, making them more advantageous among formaldehyde gas sensing techniques.

CRediT authorship contribution statement

Xiu Yang: Writing – original draft, Formal analysis, Data curation. **Baisong Chen:** Writing – original draft, Formal analysis, Conceptualization. **Yize Liang:** Investigation, Funding acquisition, Data curation. **Jiajia Hou:** Methodology, Formal analysis, Conceptualization. **Dacheng Zhang:** Supervision, Resources, Investigation. **Biao Li:** Project administration, Funding acquisition, Conceptualization. **Angelo Sampaolo:** Writing – review & editing, Investigation. **Pietro Patimisco:** Writing – review & editing, Investigation. **Vincenzo Spagnolo:** Writing – review & editing, Supervision, Funding acquisition. **Xukun Yin:** Writing – review & editing, Supervision, Investigation, Funding acquisition.

Declaration of competing interest

The authors declare that they have no known competing financial interests or personal relationships that could have appeared to influence the work reported in this paper.

Acknowledgements

This research was funded by National Natural Science Foundation of China, (grant number 62475204; 62405041; 62105252); Hangzhou Science and Technology Development Project (202204T04); Natural Science Foundation of Shaanxi Province, grant number 2023-YBGY-099; State Key Laboratory of Electrical Insulation and Power Equipment, grant number EIPE23205. The authors from PolySense Lab acknowledge financial support from Project PNC 0000001 D3-4Health Digital Driven Diagnostics, prognostics and therapeutics for sustainable Health care - CUP [B83C22006120001], The National Plan for Complementary Investments to the NRRP , Funded by the European Union – NextGenerationEU, National Recovery and Resilience Plan (NRRP), project "BRIEF—Biorobotics Research and Innovation Engineering Facilities", CUP: J13C22000400007, funded by European Union—NextGenerationEU and THORLABS GmbH, within PolySense, a joint-research laboratory.

Data availability

The data that has been used is confidential.

References

[1] P. Wolkoff, G.D. Nielsen, Non-cancer effects of formaldehyde and relevance for setting an indoor air guideline, Environ. Int. 36 (7) (2010) 788–799.
[2] D.D. Parrish, T.B. Ryerson, J. Mellqvist, J. Johansson, A. Fried, D. Richter, J. G. Walega, R.A. Washenfelder, J.A. de Gouw, J. Peischl, K.C. Aikin, S.A. McKeen, G.J. Frost, F.C. Fehsenfeld, S.C. Herndon, Primary and secondary sources of formaldehyde in urban atmospheres: Houston Texas region, Atmos. Chem. Phys. 12 (7) (2012) 3273–3288.
[3] World Health Organization. Formaldehyde. World Health Organization (1989).
[4] S. Kim, Control of formaldehyde and TVOC emission from wood-based flooring composites at various manufacturing processes by surface finishing, J. Hazard. Mater. 176 (1–3) (2010) 14–19.
[5] J.K. McLaughlin, Formaldehyde and cancer: a critical review, Int Arch Occup Environ Health 66 (1994) 295–301.
[6] N. El Zawi, A. Elyasseri, A review of toxicity, genotoxicity and teratogenicity of formaldehyde, Cancer 15 (2021) 43.
[7] T. Salthammer, S. Mentese, R. Marutzky, Formaldehyde in the indoor environment, Chem. Rev. 110 (4) (2010) 2536–2572.
[8] S.E. Ebeler, A.J. Clifford, T. Shibamoto, Quantitative analysis by gas chromatography of volatile carbonyl compounds in expired air from mice and human, J. Chromatogr. B Biomed. Sci. Appl. 702 (1–2) (1997) 211–215.
[9] P.R. Chung, C.T. Tzeng, M.T. Ke, C.Y. Lee, Formaldehyde gas sensors: a review, Sensors 13 (4) (2013) 4468–4484.
[10] M. Hladová, J. Martinka, P. Rantuch, A. Nečas, Review of spectrophotometric methods for determination of formaldehyde, Res. Papers Faculty Mater. Sci. Tech. Slovak Univ. Tech. 27 (44) (2019) 105–120.
[11] C. Liao, J. Shi, M. Zhang, R. Dalapati, Q. Tian, S. Chen, C. Wang, L. Zang, Optical chemosensors for the gas phase detection of aldehydes: mechanism, material design, and application, Mater. Adv. 2 (19) (2021) 6213–6245.
[12] L. Giarracca, L.S. Tran, S. Gosselin, B. Hanoune, L. Gasnot, Quantitative measurement of formaldehyde formed in combustion processes using gas chromatography analytical approach, Combust. Sci. Technol. 195 (12) (2023) 2716–2731.
[13] Y. Herschkovitz, I. Eshkenazi, C.E. Campbell, J. Rishpon, An electrochemical biosensor for formaldehyde, J. Electroanal. Chem. 491 (1–2) (2000) 182–187.
[14] N. Gayathri, N. Balasubramanian, Spectrophotometric determination of formaldehyde, Anal. Lett. 33 (14) (2000) 3037–3050.
[15] C. Yuan, J. Pu, D. Fu, Y. Min, L. Wang, J. Liu, UV–vis spectroscopic detection of formaldehyde and its analogs: a convenient and sensitive methodology, J. Hazard. Mater. 438 (2022) 129457.
[16] F. Li, T. Zhu, J. Yang, X. Zhang, S. Fan, S. Fu, Y. Liu, Highly sensitive formaldehyde detection using biomass hydrogel with core-shell structure, Sens. Actuators B 418 (2024) 136340.
[17] S. Kim, H.J. Kim, Comparison of standard methods and gas chromatography method in determination of formaldehyde emission from MDF bonded with formaldehyde-based resins, Bioresour. Technol. 96 (13) (2005) 1457–1464.

[18] H. Zhu, J. She, M. Zhou, X. Fan, Rapid and sensitive detection of formaldehyde using portable 2-dimensional gas chromatography equipped with photoionization detectors, Sens. Actuators B 283 (2019) 182–187.
[19] Y. Yang, Y. Hao, L. Huang, Y. Luo, S. Chen, M. Xu, W. Chen, Recent advances in electrochemical sensors for formaldehyde, Molecules 29 (2) (2024) 327.
[20] J. Chen, Y. Ling, X. Yuan, Y. He, S. Li, G. Wang, Z. Zhang, G. Wang, Highly sensitive detection of formaldehyde by laser-induced graphene-coated silver nanoparticles electrochemical sensing electrodes, Langmuir 39 (36) (2023) 12762–12773.
[21] B. Fu, C. Zhang, W. Lyu, J. Sun, C. Shang, Y. Cheng, L. Xu, Recent progress on laser absorption spectroscopy for determination of gaseous chemical species, Appl. Spectrosc. Rev. 57 (2) (2022) 112–152.
[22] M.N. Fiddler, I. Begashaw, M.A. Mickens, M.S. Collingwood, Z. Assefa, S. Bililign, Laser spectroscopy for atmospheric and environmental sensing, Sensors 9 (12) (2009) 10447–10512.
[23] A. Ancona, V. Spagnolo, P.M. Lugara, M. Ferrara, Optical sensor for real-time monitoring of CO_2 laser welding process, Appl. Opt. 40 (33) (2001) 6019–6025.
[24] F. Wan, R. Wang, H. Ge, W. Kong, H. Sun, H. Wu, G. Zhao, W. Ma, W. Chen, Optical feedback frequency locking, impact of directly reflected field and responding strategies, Optics 32 (7) (2024) 12428–12437.
[25] C.T. Zheng, W.L. Ye, G.L. Li, X. Yu, C.X. Zhao, Z.W. Song, Y.D. Wang, Performance enhancement of a mid-infrared CH4 detection sensor by optimizing an asymmetric ellipsoid gas-cell and reducing voltage-fluctuation: theory, design and experiment, Sens. Actuators B 160 (1) (2011) 389–398.
[26] W. Ren, W. Jiang, F.K. Tittel, Single-QCL-based absorption sensor for simultaneous trace-gas detection of CH 4 and N 2 O, Appl. Phys. B 117 (2014) 245–251.
[27] H. Ge, W. Kong, R. Wang, G. Zhao, W. Ma, W. Chen, F. Wan, Simple technique of coupling a diode laser into a linear power buildup cavity for Raman gas sensing, Opt. Lett. 48 (8) (2023) 2186–2189.
[28] H. Zheng, M. Lou, L. Dong, H. Wu, W. Ye, X. Yin, C.S. Kim, M. Kim, W.W. Bewley, C.D. Merritt, C.L. Canedy, M.V. Warren, I. Vurgaftman, J.R. Meyer, F.K. Tittel, Compact photoacoustic module for methane detection incorporating interband cascade light emitting device, Opt. Express 25 (14) (2017) 16761–16770.
[29] C.T. Zheng, W.L. Ye, J.Q. Huang, T.S. Cao, M. Lv, J.M. Dang, Y.D. Wang, Performance improvement of a near-infrared CH4 detection device using wavelet-denoising-assisted wavelength modulation technique, Sens. Actuators B 190 (2014) 249–258.
[30] X. Liu, Y. Ma, Sensitive carbon monoxide detection based on light-induced thermoelastic spectroscopy with a fiber-coupled multipass cell, Chin. Opt. Lett. 20 (3) (2022) 031201.
[31] Y. Pan, J. Zhao, P. Lu, C. Sima, D. Liu, Recent advances in light-induced thermoelastic spectroscopy for gas sensing: a review, Remote Sens. (Basel) 15 (1) (2022) 69.
[32] X. Yin, H. Wu, L. Dong, B. Li, W. Ma, L. Zhang, W. Yin, L. Xiao, S. Jia, F.K. Tittel, Ppb-level SO2 photoacoustic sensors with a suppressed absorption–desorption effect by using a 7.41 μm external-cavity quantum cascade laser, ACS Sensors 5 (2) (2020) 549–556.
[33] H. Cheng, F. Zeng, X. Zhang, J. Tang, Y. Zhang, The effect of the photoacoustic Field-Photoacoustic cell coupling term on the performance of the gas detection system, Opt. Laser Technol. 153 (2022) 108211.
[34] Y. Ma, G. Yu, J. Zhang, H. Luo, X. Yu, C.B. Yang, Z. Yang, R. Sun, D.Y. Chen, Research on real-time trace gas detection system based on QEPAS, Spectrosc. Spectr. Anal. 35 (11) (2015) 3003–3006.
[35] Y. Ma, Y. He, X. Yu, G. Yu, J.B. Zhang, R. Sun, Research on high sensitivity detection of carbon monoxide based on quantum cascade laser and quartz-enhanced photoacoustic spectroscopy, Acta Phys. Sin. 65 (06) (2016) 65–70.
[36] V. Spagnolo, A.A. Kosterev, L. Dong, R. Lewicki, F.K. Tittel, NO trace gas sensor based on quartz-enhanced photoacoustic spectroscopy and external cavity quantum cascade laser, Appl. Phys. B 100 (2010) 125–130.
[37] X. Yin, L. Dong, H. Wu, H. Zheng, W. Ma, L. Zhang, W. Yin, S. Jia, F.K. Tittel, Sub-ppb nitrogen dioxide detection with a large linear dynamic range by use of a differential photoacoustic cell and a 3.5 W blue multimode diode laser, Sens. Actuators B 247 (2017) 329–335.
[38] V. Spagnolo, P. Patimisco, S. Borri, G. Scamarcio, B.E. Bernacki, J. Kriesel, Part-per-trillion level SF 6 detection using a quartz enhanced photoacoustic spectroscopy-based sensor with single-mode fiber-coupled quantum cascade laser excitation, Opt. Lett. 37 (21) (2012) 4461–4463.
[39] H. Zheng, L. Dong, A. Sampaolo, H. Wu, P. Patimisco, X. Yin, W. Ma, L. Zhang, W. Yin, V. Spagnolo, S. Jia, F.K. Tittel, Single-tube on-beam quartz-enhanced photoacoustic spectroscopy, Opt. Lett. 41 (5) (2016) 978–981.
[40] M.D. Wheeler, S.M. Newman, A.J. Orr-Ewing, M.N. Ashfold, Cavity ring-down spectroscopy, J. Chem. Soc. Faraday Trans. 94 (3) (1998) 337–351.
[41] D. Romanini, I. Ventrillard, G. Méjean, J. Morville, E. Kerstel, Introduction to cavity enhanced absorption spectroscopy, Cavity-Enhanced Spectrosc. Sens. (2014) 1–60.
[42] A. O'Keefe, J.J. Scherer, J.B. Paul, CW integrated cavity output spectroscopy, Chem. Phys. Lett. 307 (5–6) (1999) 343–349.
[43] H.I. Schiff, G.I. Mackay, J. Bechara, The use of tunable diode laser absorption spectroscopy for atmospheric measurements, Res. Chem. Intermed. 20 (1994) 525–556.
[44] Y. Cao, N.P. Sanchez, W. Jiang, W. Ren, R. Lewicki, D. Jiang, R.J. Griffin, F. K. Tittel, Multi-pass absorption spectroscopy for H2O2 detection using a CW DFB-QCL, Adv. Opt. Tech. 3 (5–6) (2014) 549–558.
[45] H. Edner, P. Ragnarson, S. Spännare, S. Svanberg, Differential optical absorption spectroscopy (DOAS) system for urban atmospheric pollution monitoring, Appl. Opt. 32 (3) (1993) 327–333.
[46] T.V. Dinh, I.Y. Choi, Y.S. Son, J.C. Kim, A review on non-dispersive infrared gas sensors: improvement of sensor detection limit and interference correction, Sens. Actuators B 231 (2016) 529–538.
[47] D.C. Dumitras, D.C. Dutu, C. Matei, A.M. Magureanu, M. Petrus, C. Popa, Laser photoacoustic spectroscopy: principles, instrumentation, and characterization, J. Optoelectron. Adv. Mater. 9 (12) (2007) 3655.
[48] X. Yin, L. Dong, H. Wu, W. Ma, L. Zhang, W. Yin, L. Xiao, S. Jia, F.K. Tittel, Ppb-level H2S detection for SF6 decomposition based on a fiber-amplified telecommunication diode laser and a background-gas-induced high-Q photoacoustic cell, Appl. Phys. Lett. 111 (3) (2017) 031109.
[49] H. Cheng, J. Tang, X. Zhang, Y. Li, J. Hu, Y. Zhang, S. Mao, S. Xiao, Simultaneous detection of C_2H_2 and CO based on cantilever-enhanced photoacoustic spectroscopy, IEEE Trans. Instrum. Meas. 70 (2021) 1–10.
[50] J. D. Ingle Jr, S. R. Crouch, Spectrochemical analysis, (1988).
[51] R. Meller, G.K. Moortgat, Temperature dependence of the absorption cross sections of formaldehyde between 223 and 323 K in the wavelength range 225–375 nm, J. Geophys. Res. Atmos. 105 (D6) (2000) 7089–7101.
[52] K. Bogumil, J. Orphal, T. Homann, S. Voigt, P. Spietz, O.C. Fleischmann, A. Vogel, M. Hartmann, H. Kromminga, H. Bovensmann, J. Frerick, J.P. Burrows, Measurements of molecular absorption spectra with the SCIAMACHY pre-flight model: instrument characterization and reference data for atmospheric remote-sensing in the 230–2380 nm region, J. Photochem. Photobiol. A Chem. 157 (2–3) (2003) 167–184.
[53] I.E. Gordon, L.S. Rothman, R.J. Hargreaves, The HITRAN2020 molecular spectroscopic database, J. Quant. Spectrosc. Radiat. Transf. 277 (2022) 107949.
[54] J. Hodgkinson, R.P. Tatam, Optical gas sensing: a review, Meas. Sci. Technol. 24 (1) (2012) 012004.
[55] J.F. McClelland, Photoacoustic spectroscopy, Anal. Chem. 55 (1) (1983) 89–105.
[56] Z. Wang, Q. Wang, H. Zhang, S. Borri, I. Galli, A. Sampaolo, P. Patimisco, V. Spagnolo, P. De Natale, W. Ren, Doubly resonant sub-ppt photoacoustic gas detection with eight decades dynamic range, Photoacoustics 27 (2022) 100387.
[57] Y. Cao, Y. Xie, R. Wang, K. Liu, X. Gao, W. Zhang, Recent advances of photoacoustic spectroscopy techniques for gases sensing, J. Appl. Opt. 40 (06) (2019) 1152–1159.
[58] M. Angelmahr, A. Miklos, P. Hess, Photoacoustic spectroscopy of formaldehyde with tunable laser radiation at the parts per billion level, Appl. Phys. B 85 (2006) 285–288.
[59] A. Sampaolo, P. Patimisco, M. Giglio, A. Zifarelli, H. Wu, L. Dong, V. Spagnolo, Quartz-enhanced photoacoustic spectroscopy for multi-gas detection: a review, Anal. Chim. Acta 1202 (2022) 338894.
[60] M. Giglio, A. Elefante, P. Patimisco, A. Sampaolo, F. Sgobba, H. Rossmadl, V. Mackowiak, H. Wu, F.K. Tittel, L. Dong, V. Spagnolo, Quartz-enhanced photoacoustic sensor for ethylene detection implementing optimized custom tuning fork-based spectrophone, Opt. Express 27 (4) (2019) 4271–4280.
[61] C. Feng, M. Giglio, B. Li, A. Sampaolo, P. Patimisco, V. Spagnolo, L. Dong, H. Wu, Detection of hydrogen sulfide in sewer using an erbium-doped fiber amplified diode laser and a gold-plated photoacoustic cell, Molecules 27 (19) (2022) 6505.
[62] P. Patimisco, A. Sampaolo, L. Dong, F.K. Tittel, V. Spagnolo, Recent advances in quartz enhanced photoacoustic sensing, Appl. Phys. Rev. 5 (1) (2018).
[63] Y. Bidaux, A. Bismuto, P. Patimisco, A. Sampaolo, T. Gresch, G. Strubi, S. Blaser, F.K. Tittel, V. Spagnolo, A. Muller, J. Faist, Mid infrared quantum cascade laser operating in pure amplitude modulation for background-free trace gas spectroscopy, Opt. Express 24 (23) (2016) 26464–26471.
[64] P. Patimisco, A. Sampaolo, Y. Bidaux, A. Bismuto, M. Schott, J. Jiang, A. Muller, J. Faist, F.K. Tittel, V. Spagnolo, Purely wavelength- and amplitude-modulated quartz-enhanced photoacoustic spectroscopy, Opt. Express 24 (23) (2016) 25943–25954.
[65] P. Patimisco, G. Scamarcio, F.K. Tittel, V. Spagnolo, Quartz-enhanced photoacoustic spectroscopy: a review, Sensors 14 (4) (2014) 6165–6206.
[66] M. Giglio, A. Zifarelli, A. Sampaolo, G. Menduni, A. Elefante, R. Blanchard, C. Pfluegl, M.F. Witinski, D. Vakhshoori, H. Wu, V.M.N. Passaro, P. Patimisco, F. K. Tittrl, L. Dong, V. Spagnolo, Broadband detection of methane and nitrous oxide using a distributed-feedback quantum cascade laser array and quartz-enhanced photoacoustic sensing, Photoacoustics 17 (2020) 100159.
[67] Q. Wang, Z. Wang, W. Ren, P. Patimisco, A. Sampaolo, V. Spagnolo, Fiber-ring laser intracavity QEPAS gas sensor using a 7.2 kHz quartz tuning fork, Sens. Actuators B 268 (2018) 512–518.
[68] M. Horstjann, Y.A. Bakhirkin, A.A. Kosterev, R.F. Curl, F.K. Tittel, C.M. Wong, C. J. Hill, R.Q. Yang, Formaldehyde sensor using interband cascade laser based quartz-enhanced photoacoustic spectroscopy, Appl. Phys. B 79 (2004) 799–803.
[69] P. Patimisco, A. Sampaolo, H. Zheng, L. Dong, F.K. Tittel, V. Spagnolo, Quartz-enhanced photoacoustic spectrophones exploiting custom tuning forks: a review, Adv. Phys.: X 2 (1) (2017) 169–187.
[70] S. Dello Russo, M. Giglio, A. Sampaolo, P. Patimisco, G. Menduni, H. Wu, L. Dong, V.M.N. Passaro, V. Spagnolo, Acoustic coupling between resonator tubes in quartz-enhanced photoacoustic spectrophones employing a large prong spacing tuning fork, Sensors 19 (19) (2019) 4109.
[71] Y. Yin, D. Ren, C. Li, R. Chen, J. Shi, Cantilever-enhanced photoacoustic spectroscopy for gas sensing: a comparison of different displacement detection methods, Photoacoustics (2022) 100423.
[72] C.B. Hirschmann, J. Lehtinen, J. Uotila, S. Ojala, R.L. Keiski, Sub-ppb detection of formaldehyde with cantilever enhanced photoacoustic spectroscopy using quantum cascade laser source, Appl. Phys. B 111 (2013) 603–610.

[73] X. Wang, K. Wang, J. Yu, H. Jia, Z. Mo, J. Wang, J. Tang, X. Fang, Z. Wei, Application of cavity ring-down spectroscopy in trace gas detection, Sci. Tech. Eng. 17 (14) (2017) 120–130.
[74] Y. Mi, X. Wang, S. Zhan, Review on cavity ring down spectroscopy technology and its application, Optical Instruments (05) (2007), 85-89.
[75] H. Dahnke, G. Von Basum, K. Kleinermanns, P. Hering, M. Mürtz, Rapid formaldehyde monitoring in ambient air by means of mid-infrared cavity leak-out spectroscopy, Appl. Phys. B 75 (2002) 311–316.
[76] W. Zhou, Z. Ren, B. Peng, Measurement of formaldehyde in gas mixture using cavity ring-down spectroscopy, J. Zhejiang Normal Univ.(Nat. Sci.) 01 (2007) 11–15.
[77] X. Chao, Z. Hu, N. Zhu, Research and application progress of cavity-enhanced absorption spectroscopy (Invited), Acta Photonica Sinica 52 (3) (2023) 0352102.
[78] L. Han, H. Xia, F. Dong, Z. Zhang, T. Pang, P. Sun, B. Wu, X. Cui, Z. Li, R. Yu, Progress and application of cavity enhanced absorption spectroscopy technology, Chinese J. Lasers 45 (09) (2018) 43–54.
[79] Q. He, C. Zheng, M. Lou, W. Ye, Y. Wang, F.K. Tittel, Dual-feedback mid-infrared cavity-enhanced absorption spectroscopy for H 2 CO detection using a radio-frequency electrically-modulated interband cascade laser, Opt. Express 26 (12) (2018) 15436–15444.
[80] Q. He, J. Li, Q. Feng, Development of a mid-infrared cavity enhanced formaldehyde detection system, Spectrosc. Spectr. Anal. 41 (07) (2021) 2077–2081.
[81] E. J. Moyer, D. S. Sayres, G. S. Engel, J. M. St. Clair, F. N. Keutsch, N. T. Allen, J. H. Kroll, J. G. Anderson, Design considerations in high-sensitivity off-axis integrated cavity output spectroscopy. Applied Physics B 92 (2008), 467-474.
[82] J.H. Miller, Y.A. Bakhirkin, T. Ajtai, F.K. Tittel, C.J. Hill, R.Q. Yang, Detection of formaldehyde using off-axis integrated cavity output spectroscopy with an interband cascade laser, Appl. Phys. B 85 (2006) 391–396.
[83] G. Li, Y. Song, K. Ma, X. Zhang, H. Zhao, Z. Zhang, Y. Liu, Y. Wu, J. Li, S. Zhai, Q. Li, K. Zheng, C. Zheng, WM-OA-ICOS based mid-infrared dual-range real-time trace sensor for formaldehyde detection in exhaled breath, IEEE Sens. J. 23 (1) (2022) 274–284.
[84] B. ISAC, Differential optical absorption spectroscopy (DOAS), (1994).
[85] C. Yang, Detection of indoor air quality based on DOAS technique, J. Hubei Inst. Nationalities (Nat. Sci. Ed.) 01 (2007) 68–70.
[86] M. Qin, X. Zhang, M. Chang, Detection technology of formaldehyde gas concentration based on infrared absorption spectroscopy, Opt. Instruments 39 (03) (2017) 6–10.
[87] Q. Liu, Z. Wang, J. Chen, Research Progress of TDLAS in Atmospheric Detection, Electro-optic Technology Application 36 (06) (2021), 24-27+70.
[88] Y. Hu, R. Cui, H. Wu, L. Dong, Design and progress of miniature milti-pass cells, Chinese J. Quantum Electron. 38 (05) (2021) 608–616.
[89] G.W. Harris, G.I. Mackay, T. Iguchi, L.K. Mayne, H.I. Schiff, Measurements of formaldehyde in the troposphere by tunable diode laser absorption spectroscopy, J. Atmos. Chem. 8 (1989) 119–137.
[90] P. Werle, A. Popov, Application of antimonide lasers for gas sensing in the 3–4-μm range, Appl. Opt. 38 (9) (1999) 1494–1501.
[91] Y. Mine, N. Melander, D. Richter, D.G. Lancaster, K.P. Petrov, R.F. Curl, F. K. Tittel, Detection of formaldehyde using mid infrared difference-frequency generation, Appl. Phys.-Sec. B-Lasers Opt. 65 (6) (1997) 771–774.
[92] K. Tanaka, K. Miyamura, K. Akishima, K. Tonokura, M. Konno, Sensitive measurements of trace gas of formaldehyde using a mid-infrared laser spectrometer with a compact multi-pass cell, Infrared Phys. Technol. 79 (2016) 1–5.
[93] S. Li, L. Dong, H. Wu, X. Yin, W. Ma, L. Zhang, W. Yin, A. Sampaolo, P. Patimisco, V. Spagnolo, S. Jia, F.K. Tittel, Simultaneous multi-gas detection between 3 and 4 μm based on a 2.5-m multipass cell and a tunable Fabry-Pérot filter detector, Spectrochim. Acta A Mol. Biomol. Spectrosc. 216 (2019) 154–160.
[94] D.G. Lancaster, A. Fried, B. Wert, B. Henry, F.K. Tittel, Difference-frequency-based tunable absorption spectrometer for detection of atmospheric formaldehyde, Appl. Opt. 39 (24) (2000) 4436–4443.
[95] D. Rehle, D. Leleux, M. Erdelyi, F. Tittel, M. Fraser, S. Friedfeld, Ambient formaldehyde detection with a laser spectrometer based on difference-frequency generation in PPLN, Appl. Phys. B 72 (2001) 947–952.
[96] D. Richter, A. Fried, B.P. Wert, J.G. Walega, F.K. Tittel, Development of a tunable mid-IR difference frequency laser source for highly sensitive airborne trace gas detection, Appl. Phys. B 75 (2002) 281–288.
[97] J. Li, U. Parchatka, H. Fischer, A formaldehyde trace gas sensor based on a thermoelectrically cooled CW-DFB quantum cascade laser, Anal. Methods 6 (15) (2014) 5483–5488.
[98] M. Winkowski, T. Stacewicz, Optical detection of formaldehyde in air in the 3.6 μm range, Biomed. Opt. Express 11 (12) (2020) 7019–7031.
[99] W. Ren, L. Luo, F.K. Tittel, Sensitive detection of formaldehyde using an interband cascade laser near 3.6 μm, Sen. Actuators B Chem. 221 (2015) 1062–1068.
[100] L. Dong, Y. Yu, C. Li, S. So, F.K. Tittel, Ppb-level formaldehyde detection using a CW room-temperature interband cascade laser and a miniature dense pattern multipass gas cell, Opt. Express 23 (15) (2015) 19821–19830.
[101] K. Duan, J. Wu, T. Grabe, R. Lachmayer, W. Ren, A portable ppb-level formaldehyde sensor for real-time air quality monitoring, IEEE Trans. Instrum. Meas. 73 (2023).
[102] T. Wu, R. Hu, P. Xie, L. Zhang, C. Hu, X. Liu, J. Wang, L. Zhong, J. Tong, W. Liu, A Mid-infrared quantum cascade laser ultra-sensitive trace formaldehyde detection system based on improved dual-incidence multipass gas cell, Sensors 23 (12) (2023) 5643.
[103] B. Fang, N. Yang, C. Wang, W. Zhao, H. Zhou, W. Zhang, Highly sensitive portable laser absorption spectroscopy formaldehyde sensor using compact spherical mirror multi-pass cell, Sens. Actuators B 394 (2023) 134379.
[104] M. Boutonnat, D.A. Gilmore, K.A. Keilbach, N. Oliphant, G.H. Atkinson, Photoacoustic detection of formaldehyde as a minority component in gas mixtures, Appl. Spectrosc. 42 (8) (1988) 1520–1524.
[105] J.J. Davenport, J. Hodgkinson, J.R. Saffell, R.P. Tatam, Formaldehyde sensor using non-dispersive UV spectroscopy at 340nm, Opt. Sens. Detection III SPIE 9141 (2014) 119–124.
[106] R.K. Jha, Non-dispersive infrared gas sensing technology: a review, IEEE Sens. J. 22 (1) (2021) 6–15.
[107] P. Nau, J. Koppmann, A. Lackner, A. Brockhinke, Detection of formaldehyde in flames using UV and MIR absorption spectroscopy, Zeitschrift Für Physikalische Chemie 229 (4) (2015) 483–494.
[108] S. Shen, S. Wang, B. Zhou, Investigation of atmospheric formaldehyde and glyoxal based on differential optical absorption spectroscopy, Spectrosc. Spectr. Anal. 36 (08) (2016) 2384–2390.
[109] R. Sheng, J. Xiang, S. Lu, Research on CH_2O Emission Detection Based on Industrial Process of Ultraviolet Difference Optical Spectrum Technology, China Environmental Protection Industry (09) (2019), 65-68.
[110] R.A. Washenfelder, A.R. Attwood, J.M. Flores, K.J. Zarzana, Y. Rudich, S. S. Brown, Broadband cavity-enhanced absorption spectroscopy in the ultraviolet spectral region for measurements of nitrogen dioxide and formaldehyde, Atmos. Meas. Tech. 9 (1) (2016) 41–52.
[111] J. Liu, X. Li, Y. Yang, H. Wang, C. Kuang, Y. Zhu, M. Chen, J. Hu, L. Zeng, Y. Zhang, Sensitive detection of ambient formaldehyde by incoherent broadband cavity enhanced absorption spectroscopy, Anal. Chem. 92 (3) (2020) 2697–2705.
[112] A.A. Kosterev, Y.A. Bakhirkin, R.F. Curl, F.K. Tittel, Quartz-enhanced photoacoustic spectroscopy, Opt. Lett. 27 (21) (2002) 1902–1904.